Research article

Journal of Molecular Recognition

Received: 30 June 2015, Revised: 24 September 2015, Accepted: 30 September 2015, Published online in Wiley Online Library: 4 November 2015

(wileyonlinelibrary.com) DOI: 10.1002/jmr.2514

Elucidation of the effect of aptamer immobilization strategies on the interaction between cell and its aptamer using atomic force spectroscopy

Qing Wang, Bianxia Luo, Xiaohai Yang*, Kemin Wang*, Lin Liu, Shasha Du and Zhiping Li

The immobilization strategy of cell-specific aptamers is of great importance for studying the interaction between a cell and its aptamer. However, because of the difficulty of studying living cell, there have not been any systematic reports about the effect of immobilization strategies on the binding ability of an immobilized aptamer to its target cell. Because atomic force spectroscopy (AFM) could not only be suitable for the investigation of living cell under physiological conditions but also obtains information reflecting the intrinsic properties of individuals, the effect of immobilization strategies on the interaction of aptamer/human hepatocarcinoma cell Bel-7404 was successively evaluated using AFM here. Two different immobilization methods, including polyethylene glycol immobilization method and glutaraldehyde immobilization method were used, and the factors, such as aptamer orientation, oligodeoxythymidine spacers and dodecyl spacers, were investigated. Binding events measured by AFM showed that a similar unbinding force was obtained regardless of the change of the aptamer orientation, the immobilization method, and spacers, implying that the biophysical characteristics of the aptamer at the molecular level remain undisturbed. However, it showed that the immobilization orientation, immobilization method, and spacers could alter the binding probability of aptamer/Bel-7404 cell. Presumably, these factors may affect the accessibility of the aptamer toward its target cell. These results may provide valuable information for aptamer sensor platforms including ultrasensitive biosensor design.

Additional supporting information may be found in the online version of this article at the publisher's web site.

Keywords: single-molecule force spectroscopy; aptamer orientation; oligo(dT) spacers; dodecyl spacers

INTRODUCTION

Sensitive and specific identification of cancer cells is of great importance to achieve early diagnosis and accurate therapy for cancer (Balic *et al.*, 2013; Schwarzenbach *et al.*, 2014). Recently, owing to their high binding affinity, high specificity, non-toxicity, easily modified chemical structure, and wide range of targets, aptamers have shown great potential for the application of cancer cell recognition (Fang and Tan, 2009; Tan *et al.*, 2013). As recognition probes, aptamers are usually immobilized on a solid surface. To maintain the binding affinity and specificity that the aptamer displays in solution, immobilization strategy of aptamer is very important (Balamurugan *et al.*, 2008; Walter *et al.*, 2008). Some technologies, such as surface plasmon resonance (SPR) (Baldrich *et al.*, 2004; Balamurugan *et al.*, 2006), quartz crystal microbalance (QCM) (Bini *et al.*, 2007; Zhang and Yadavalli, 2011), and fluorescent method (Cho *et al.*, 2006; Katilius *et al.*, 2007; Lao *et al.*, 2009), were used to explore the effect of the immobilization parameters of aptamer on the binding ability of aptamer to its target. It was found that optimizing those simple but sometimes easily neglected steps, such as orientation and spacer, was of paramount importance and could obtain significant improvements in analytical performances (Guo *et al.*, 1994; Lao *et al.*, 2009). However, because of the difficulty of studying living cell, systematic studies about the effect of immobilization strategies on the binding ability of the immobilized aptamer to its target cell have not been reported.

Compared with the aforementioned methods, such as SPR or QCM, atomic force spectroscopy (AFM)-based single-molecule force spectroscopy (SMFS) could obtain information reflecting the intrinsic properties of individuals that might be hidden in the measurements by traditional ensemble techniques (Shan and Wang, 2015; Wang and Yadavalli, 2014; Wang *et al.*, 2015; Zhao *et al.*, 2012). Generally, for those researches that the effects of immobilization parameters of aptamers were investigated using SPR or QCM technology, the influence of the surface density of an aptamer has to be considered, resulting

* *Correspondence to: K. Wang and X. Yang, State Key Laboratory of Chemo/Biosensing and Chemometrics, College of Chemistry and Chemical Engineering, Key Laboratory for Bio-Nanotechnology and Molecular Engineering of Hunan Province, Hunan University, Changsha 410082, China.*
E-mail: kmwang@hnu.edu.cn; yangxiaohai@hnu.edu.cn

Q. Wang, B. Luo, X. Yang, K. Wang, L. Liu, S. Du, Z. Li
State Key Laboratory of Chemo/Biosensing and Chemometrics, College of Chemistry and Chemical Engineering, Key Laboratory for Bio-Nanotechnology and Molecular Engineering of Hunan Province, Hunan University, Changsha 410082, China

in an increased complexity in studying the effect of aptamer immobilization strategies. As for SMFS, the effect of the surface density of an aptamer is negligible because the information about intrinsic properties of individuals was obtained. That is, the biophysical differences of an aptamer immobilized by different strategies can be observed using SMFS (Zhang and Yadavalli, 2011). Furthermore, SMFS could not only obtain the biomolecular interaction with nanometer positional accuracy and piconewton force sensitivity (Jin *et al*., 2004; Yang *et al*., 2007; Steffens *et al*., 2012) but also be suitable for the investigation of living cell under physiological conditions (Formosa *et al*., 2015; Wang and Yadavalli, 2014; Wang *et al*., 2014). Therefore, SMFS has the potential to become a powerful tool to evaluate aptamer immobilization strategies at the living cell level.

Here, an aptamer against human hepatocarcinoma cell line Bel-7404, which was selected by our groups (Guo *et al*., 2013; Shi *et al*., 2013), was used as a model, and a systematic study about the effects of immobilization strategies on the interaction of aptamer/Bel-7404 cell was investigated by SMFS at the living cell level. The influence of aptamer orientation on the interaction of aptamer/Bel-7404 cell was investigated by using polyethylene glycol (PEG) or glutaraldehyde as the cross-linker, and then the effects of two types of spacers including oligodeoxythymidine (oligo(dT)) spacers (T_{10}, T_{20}, and T_{30}) and dodecyl spacers ($carbon_{12}$, $carbon_{24}$, and $carbon_{36}$) on the interaction of aptamer/Bel-7404 cell were evaluated. This work may provide valuable reference for the immobilization of aptamers in diagnostic and therapeutic applications.

MATERIALS AND METHODS

Materials

RPMI-1640 culture medium and fetal bovine serum were obtained from Gibco BRL Corporation (USA). (3-Mercaptopropyl)-trimethoxysilane and (3-aminopropyl)triethoxysilane were obtained from Sigma-Aldrich (USA). Glutaraldehyde was obtained from Sinopharm chemical reagent limited corporation (China). N-hydroxysuccinimide-polyethylenglycol-maleimide (NHS-PEG-MAL, MW 3400) was purchased from Nanocs (USA). Human hepatocarcinoma cell line Bel-7404, human normal liver cell line L-02, and human cervical carcinoma cell line HeLa were purchased from Shanghai Institutes for Biological Science (China). Human hepatocellular carcinoma cell line SMMC-7721 and human cholangiocarcinoma cell line QBC-939 were purchased from Xiangya School of Medicine, Central South University (China). The aptamer with the highest affinity (i.e. the dissociation constant was 44.4 ± 3.1 nM) was used according to our previous work (Guo *et al*., 2013), and aptamers listed in Table 1 were synthesized by Shangon Biotech (Shanghai, China). All reagents used in the experiments were analytical grade.

Cell culture

According to our previous work (Wang *et al*, 2014), all cells were cultured in RPMI 1640 medium containing 15% fetal bovine serum and then were maintained in an incubator at 37 °C with 5% CO_2. Next, the cells were seeded on 35 mm dish at a final cell density of 5×10^4 cells per milliliter for 24–36 h. Before experiments, the subconfluent cells (about 80–90%) were rinsed four times using 2 ml 0.01 M phosphate-buffered saline (PBS) buffer (pH 7.4), and then 2.5 ml RPMI 1640 medium without fetal bovine serum was added.

Modification of atomic force spectroscopy tips

The AFM tips (Si_3N_4, Benyuan Nano Instrument Co., China) were first cleaned according to the previous work (Wang *et al*., 2015). Then aptamers were modified on the AFM tips using two conventional immobilization methods, that is, using PEG (Kienberger *et al*., 2006; Zhao *et al*., 2013) or glutaraldehyde (Khezrian *et al*., 2013; Luo *et al*., 2013) as the cross-linker (Figure 1(A)).

(1) *PEG immobilization method*. The cleaned tips were silanized with 1.0% (v/v) (3-Mercaptopropyl)trimethoxysilane in toluene for 2 h at room temperature and then rinsed thoroughly with toluene. The silanized tips were activated by incubating with 1 mg/ml of NHS-PEG-MAL in dimethylsulfoxide for 3 h at room temperature, followed by thoroughly rinsing with dimethylsulfoxide to remove any unbound NHS-PEG-MAL. The activated tips were incubated with 100 nM aptamer for 1 h at room temperature. After rising with 0.01 M PBS

Table 1. Aptamer sequence

Name	Sequence
5′-ls2n	5′-NH_2-ATG GAA TGT GGG AGG GGG ACT CAG GAC AGT CAC GGG A-3′
3′-ls2n	5′- ATG GAA TGT GGG AGG GGG ACT CAG GAC AGT CAC GGG A-NH_2-3′
5′-T_{10}-ls2n	5′-NH_2-T_{10}-ATG GAA TGT GGG AGG GGG ACT CAG GAC AGT CAC GGG A-3′
5′-T_{20}-ls2n	5′-NH_2-T_{20}-ATG GAA TGT GGG AGG GGG ACT CAG GAC AGT CAC GGG A-3′
5′-T_{30}-ls2n	5′-NH_2-T_{30}-ATG GAA TGT GGG AGG GGG ACT CAG GAC AGT CAC GGG A-3′
3′-T_{10}-ls2n	5′-ATG GAA TGT GGG AGG GGG ACT CAG GAC AGT CAC GGG A-T_{10}-NH_2-3′
3′-T_{20}-ls2n	5′-ATG GAA TGT GGG AGG GGG ACT CAG GAC AGT CAC GGG A-T_{20}-NH_2-3′
3′-T_{30}-ls2n	5′-ATG GAA TGT GGG AGG GGG ACT CAG GAC AGT CAC GGG A-T_{30}-NH_2-3′
5′-$carbon_{12}$-ls2n	5′-NH_2-$(CH_2)_{12}$-ATG GAA TGT GGG AGG GGG ACT CAG GAC AGT CAC GGG A-3′
5′-$carbon_{24}$-ls2n	5′-NH_2-$(CH_2)_{24}$-ATGG AAT GTG GGA GGG GGA CTC AGG ACA GTC ACG GGA-3′
5′-$carbon_{36}$-ls2n	5′-NH_2-$(CH_2)_{36}$-ATG GAA TGT GGG AGG GGG ACT CAG GAC AGT CAC GGG A-3′
3′-$carbon_{12}$-ls2n	5′-ATG GAA TGT GGG AGG GGG ACT CAG GAC AGT CAC GGG A-$(CH_2)_{12}$-NH_2-3′
3′-$carbon_{24}$-ls2n	5′-ATG GAA TGT GGG AGG GGG ACT CAG GAC AGT CAC GGG A-$(CH_2)_{24}$-NH_2-3′
3′-$carbon_{36}$-ls2n	5′-ATG GAA TGT GGG AGG GGG ACT CAG GAC AGT CAC GGG A-$(CH_2)_{36}$-NH_2-3′
Random DNA	5′-NH_2-$(N)_{37}$-3′[a]

[a]N was random base.

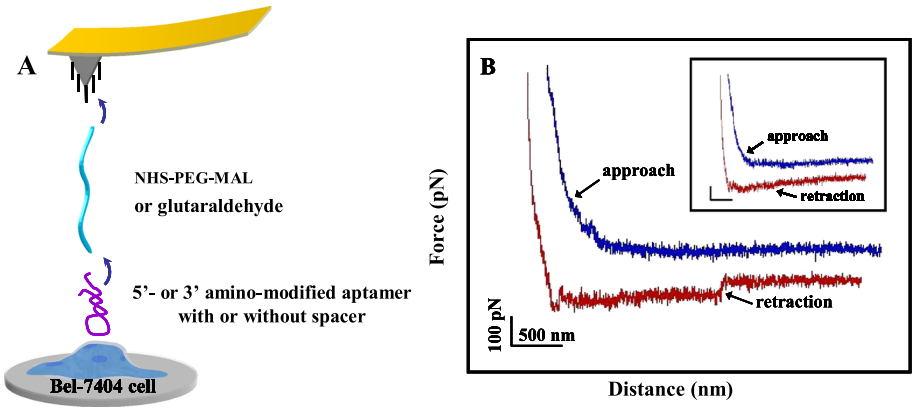

Figure 1. (A) Schematic diagram of single-molecule force measurements on Bel-7404 cells with different aptamer-modified atomic force spectroscopy tip. (B) Typical force–distance curves with aptamer-modified atomic force spectroscopy tip and Bel-7404 cells. The specific unbinding events vanished as Bel-7404 cell was blocked using 500 nM aptamer (insert). NHS-PEG-MAL, N-hydroxysuccinimide-polyethylenglycol-maleimide.

(pH 7.4), the aptamer-modified tips were stored in 0.01 M PBS at 4 °C until use.

(2) *Glutaraldehyde immobilization method.* The cleaned tips were silanized with 1.0% (v/v) (3-aminopropyl)triethoxysilane in toluene for 2 h at room temperature and then rinsed thoroughly with toluene. The silanized tips were activated by incubating with 10% glutaraldehyde solution in 0.01 M PBS buffer (pH 7.4) for 1 h at room temperature, followed by thoroughly rinsing with 0.01 M PBS buffer (pH 7.4). The activated tips were incubated with 100 nM aptamer for 1 h at room temperature. After rinsing with 0.01 M PBS (pH 7.4), the aptamer-modified tips were stored in 0.01 M PBS (pH 7.4) at 4 °C until use.

Atomic force spectroscopy measurement

All force measurements were performed in freshly prepared RPMI 1640 medium at room temperature using the JPK biological atomic force microscopy (JPK Instruments AG, Germany). The spring constants of the tips were in the range of 0.085–0.087 N/m, determined by the thermal fluctuation method (Butt and Jaschke, 1995). The force curves were recorded and analyzed by JPK NanoWizard® SPM software.

As shown in Figure 1(A), the amino-modified aptamer was first immobilized on the AFM tip through different immobilization strategies. Then, aptamer-functionalized AFM tip was used to approach the Bel-7404 cell, allowed to dwell on the substrate and then retracted from the substrate. The surface density of the aptamer on the AFM tips was adjusted by altering the concentration of aptamer to ensure that statistically only one binding pair could be formed in the contact area. For statistical evaluation, more than 1000 force–distance cycles were collected from each experiment. Well-defined force–distance curves were recorded with configurations displayed in Figure 1(B). The first peak that occurred randomly was caused by the nonspecific force between the tip and substrate, whereas the second peak represented the specific force between the putative receptor and aptamer. The second peak appeared at about 1–3.5 μm away from the separation of tip and cell (Panorchan *et al.*, 2006). It was also verified using blocking experiment. Bel-7404 cells were first blocked using 500 nM aptamer, and then the force–distance curves between aptamer-functionalized AFM tip and the blocked Bel-7404 cell were recorded. The results showed that the first peak did not change but the second peak disappeared (the inset of Figure 1 (B)). It was implied that the second peak resulted from the specific interaction of the aptamer and Bel-7404 cell. Therefore, the second peak was counted for the following analyses. The detected binding events of Bel-7404 cell and its aptamer were analyzed to obtain the average binding forces and the binding probabilities, which were determined as the probability for observation of unbind events in all force–distance cycles.

RESULTS AND DISCUSSIONS

The dependence of single-molecular force between the aptamer and A549 cell on loading rate

According to the Bell model (Bell, 1978), the most probable unbinding force (F) is dependent on the logarithm of the loading rate (r) as the following (Equation 1):

$$F = \frac{k_B T}{\chi_\beta} \ln\left(\frac{r\chi_\beta}{k_{off}(0)k_B T}\right) = \frac{k_B T}{\chi_\beta} \ln r + \frac{k_B T}{\chi_\beta} \ln\left(\frac{x_\beta}{k_{off}(0)k_B T}\right) \quad (1)$$

where $k_{off}(0)$ is the dissociation rate constant at zero force, χ_β is the distance from the energy minimum of the bound state to the activation barrier, k_B is the Boltzmann constant, and T is the absolute temperature. Here, we first measured the unbinding forces between the Bel-7404 cell and aptamer (5′-1s2n) at the loading rates ranging from 8.5×10^4 to 3.4×10^6 pN/s. As shown in Figure 2(A), the unbinding force of 5′-1s2n/Bel-7404 cell interaction varied in the range of 60–120 pN and linearly increased with the logarithm of the loading rate. From the slope and intercept of the fit linear force region, $k_{off}(0)$ and χ_β were calculated to be 50.37 s^{-1} and 0.298 nm, respectively. In addition, the binding lifetime τ (=1/k_{off}) was estimated to be 0.02 s.

The dependence of binding probability on interaction time

The interaction time (the time of tip resting on the surface) is another parameter that may affect the unbinding force. As shown in Figure 2(B), the binding probability increased exponentially with surface interaction time in the range of 5–30% at the loading rate of 3.4×10^5 pN/s and reached a plateau after 0.6 s. Here, 0.3 s was chosen as the interaction time in the

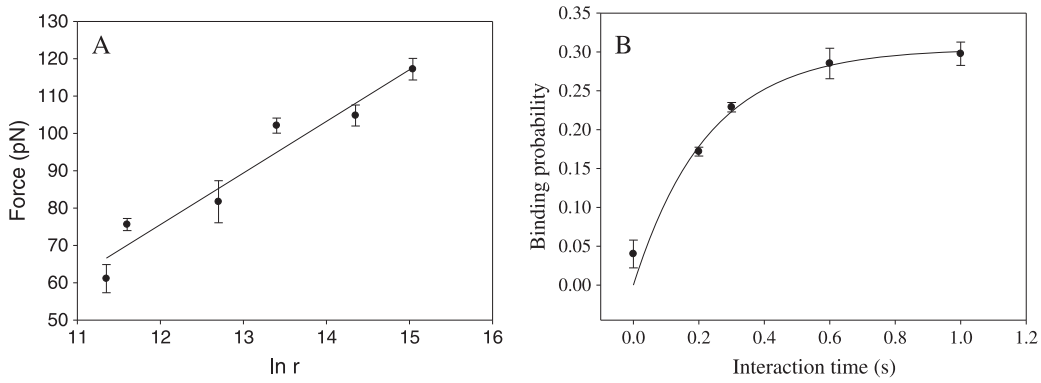

Figure 2. (A) Plot of the unbinding force for the interaction between aptamer and Bel-7404 cell against the logarithm of the loading rate. (B) Dependence of the binding probability on the surface interaction time (constant loading rate of 3.4×10^5 pN/s).

following experiments because the suitable binding probability could be obtained at 0.3 s.

Effect of immobilization orientation on the interaction of aptamer/Bel-7404 cell

The effect of immobilization orientation on the interaction between the aptamer and Bel-7404 cell was first investigated. The amino-modified aptamer was immobilized on the AFM tip through its 5′-end or 3′-end, then the interaction of 5′-end or 3′-end amino-modified aptamer/Bel-7404 cell was explored by SMFS at the loading rate of 3.4×10^5 pN/s. The results were shown in Figure 3 and Table S1. As shown in Figure 3, a single maximum in the histogram by Gaussian fitting indicated that the single-molecule forces were measured. Similar force distributions were obtained for 5′-end immobilization and 3′-end immobilization. Take PEG immobilization for example, for 5′-end amino-modified aptamer, the unbinding force was 81.73 ± 5.63 pN and the binding probability was 22.89 ± 0.61% for aptamer/Bel-7404 cell at the loading rate of 3.4×10^5 pN/s (Curve 1 in Figure 3(A)). For 3′-end amino-modified aptamer, similar unbinding force (82.90 ± 2.87 pN) was obtained. However, the binding probability (14.17 ± 3.16%) was much lower than that of 5′-end amino-modified aptamer/Bel-7404 cell (22.89 ± 0.61%) (Figure 4). Similar results could be obtained when glutaraldehyde was used as the cross-linker (Figure 4). Because similar unbinding force distributions were obtained regardless of 3′-end or 5′-end immobilization, it can be concluded that the biophysical characteristics of the aptamer at the molecular level were not influenced by the immobilization orientation. Furthermore, the results showed that immobilization through the aptamer 5′-end improved the binding of aptamer to Bel-7404 cell compared with immobilization through the 3′-end. It suggested that either 3′-end modification/immobilization interfered with the correct folding of this aptamer, thus influencing its ability to bind Bel-7404 cell, or, alternatively, that 5′-end modification improved structural stability (Baldrich *et al.*, 2004).

In addition, for immobilization through 3′-end or 5′-end amino-modified aptamer, the binding probability of aptamer/Bel-7404 cell using PEG as the cross-linker was higher than that of using glutaraldehyde as the cross-linker (shown in Figure 4 and Table S1). It may have resulted from the property of PEG. The average length of PEG was ~30 nm (Eckel *et al.*, 2005), which was longer than that of glutaraldehyde. It could enhance the steric flexibility as to improve the folding of aptamer for cell recognition, resulting in the increase of the binding probability.

Effect of oligodeoxythymidine spacer on the interaction of aptamer/Bel-7404 cell

The effect of oligo(dT) spacer on the interaction of aptamer/Bel-7404 cell was then investigated. When three kinds of oligo(dT)

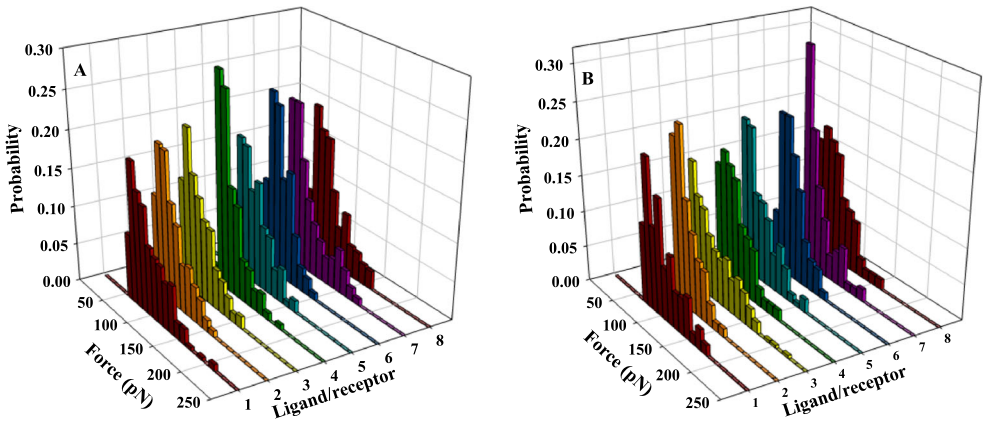

Figure 3. Force distribution of different aptamers functionalized atomic force spectroscopy tip toward Bel-7404 cell at the constant loading rate of 3.4×10^5 pN/s. (A) Using polyethylene glycol as the cross-linker; (B) using glutaraldehyde as the cross-linker. (1) 5′-1s2n; (2) 5′-T_{10}-ls2n; (3) 5′-T_{20}-ls2n; (4) 5′-T_{30}-ls2n; (5) 3′-1s2n; (6) 3′-T_{10}-ls2n; (7) 3′-T_{20}-ls2n; (8) 3′-T_{30}-ls2n.

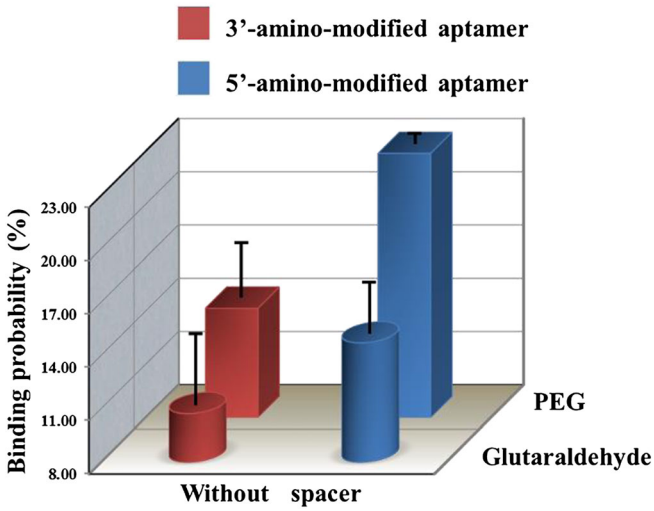

Figure 4. Effect of immobilization orientation on the binding probability of 3′- or 5′-amino-modified aptamer/Bel-7404 cell. The constant loading rate was 3.4×10^5 pN/s. PEG, polyethylene glycol.

spacers (T_{10}, T_{20}, and T_{30}) were respectively incorporated into the aptamer at its 3′-end or 5′-end, the interaction between the aptamer and Bel-7404 cell was measured by SMFS. In comparison with those aptamers without spacer, similar unbinding force distributions (Figure 3) were obtained for the aptamers with oligo (dT) spacers, implying that the biophysical characteristics of the aptamer at the molecular level remain undisturbed. But, the binding probability of aptamer/Bel-7404 cell increased (shown in Figure 5 and Table S1) along with the increase of oligo(dT) spacers, especially for aptamer immobilized through 3′-end. Take the immobilization of aptamer through its 3′-end using PEG as the cross-linker for example, the binding probability of aptamer/Bel-7404 cell increased from $14.17 \pm 3.16\%$ to $27.04 \pm 1.27\%$ as the length of oligo(dT) spacer increased to T_{30} (Table S1). These results demonstrated that the addition of oligo(dT) spacer could improve the affinity of the aptamer to Bel-7404 cell. Moreover, the result implied that the incorporation of an oligo(dT) spacer did not interfere with the folding of the binding motif through undesired intramolecular T–A base pairing. Presumably, the anchored aptamer molecules with a negatively charged oligo(dT) spacer were likely to repel each other to create room for target-induced folding. That is, an oligo(dT) spacer can facilitate more anchored aptamer molecules to fold into binding motifs. Thus, the oligo(dT) spacer resulted in the increase of the binding probability of aptamer/Bel-7404 cell.

In comparison with immobilization through 5′-end, the binding probability of aptamer/Bel-7404 cell dramatically increased with the increase of oligo(dT) spacers for immobilization through 3′-end (Figure 5). Presumably, it might be ascribed to the longer spacer required in the 3′-end immobilization, which facilitates the structural folding of aptamer. In comparison with PEG immobilization, incorporation of oligo(dT) spacer could dramatically improve the binding probability of aptamer/Bel-7404 cell for glutaraldehyde immobilization (Figure 5). Because the length of glutaraldehyde was shorter than that of PEG molecule, the addition of oligo(dT) spacer kept the aptamer staying far from the immobilization surface, resulting in the decrease of steric hindrance. Subsequently, it could improve the folding of aptamer for cell recognition, thereby increasing the binding probability obviously.

Effect of dodecyl spacer on the interaction of aptamer/Bel-7404 cell

Besides oligo(dT), dodecyl spacers have been used for improving the aptamer-based detection (Ali and Pichon, 2014; Lao *et al*., 2009). In this work, three kinds of dodecyl spacers ($carbon_{12}$, $carbon_{24}$, and $carbon_{36}$) were respectively incorporated into the aptamer at its 3′-end or 5′-end, then the interaction between the aptamer and Bel-7404 cell was measured by SMFS. The results were shown in Figure 6 and Table S1. As shown in Figure 6, similar histograms representing interaction forces distributions of aptamer with dodecyl spacer/Bel-7404 cell were obtained for PEG immobilization and glutaraldehyde immobilization methods, implying that the biophysical characteristics of the aptamer at the molecular level remained undisturbed. For PEG immobilization, the binding probability of aptamer/Bel-7404 cell almost kept unchanged when dodecyl spacer was incorporated into the aptamer (Figure 7). For glutaraldehyde immobilization, the binding

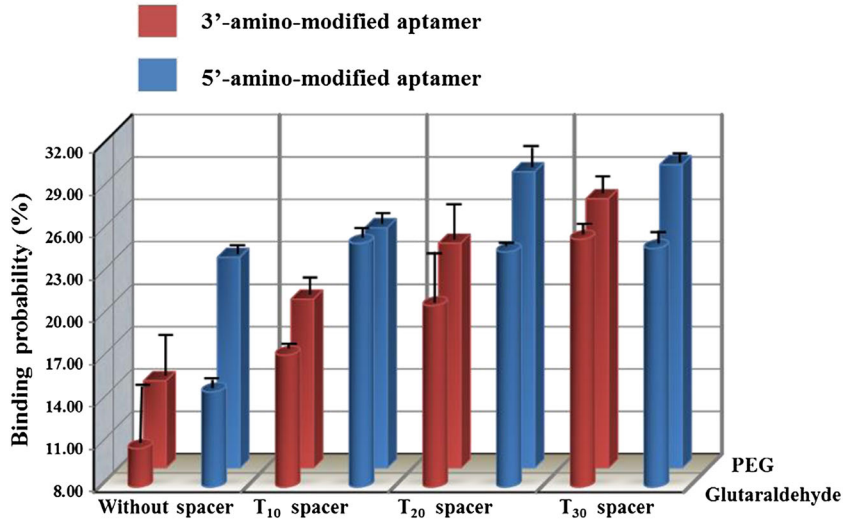

Figure 5. Effect of oligodeoxythymidine spacer on the binding probability of 3′- or 5′-amino-modified aptamer/Bel-7404 cell. The constant loading rate was 3.4×10^5 pN/s. PEG, polyethylene glycol.

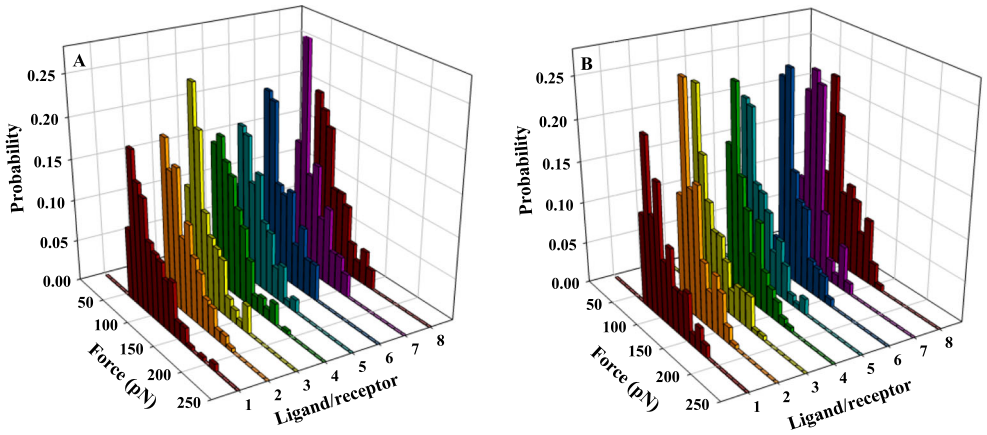

Figure 6. Force distribution of different aptamers functionalized atomic force spectroscopy tip toward Bel-7404 cell at the constant loading rate of 3.4×10^5 pN/s. (A) Using polyethylene glycol as the cross-linker; (B) using glutaraldehyde as the cross-linker. (1) 5′-1s2n; (2) 5′-carbon$_{12}$-ls2n; (3) 5′-carbon$_{24}$-ls2n; (4) 5′-carbon$_{36}$-ls2n; (5) 3′-1s2n; (6) 3′-carbon$_{12}$-ls2n; (7) 3′-carbon$_{24}$-ls2n; (8) 3′-carbon$_{36}$-ls2n.

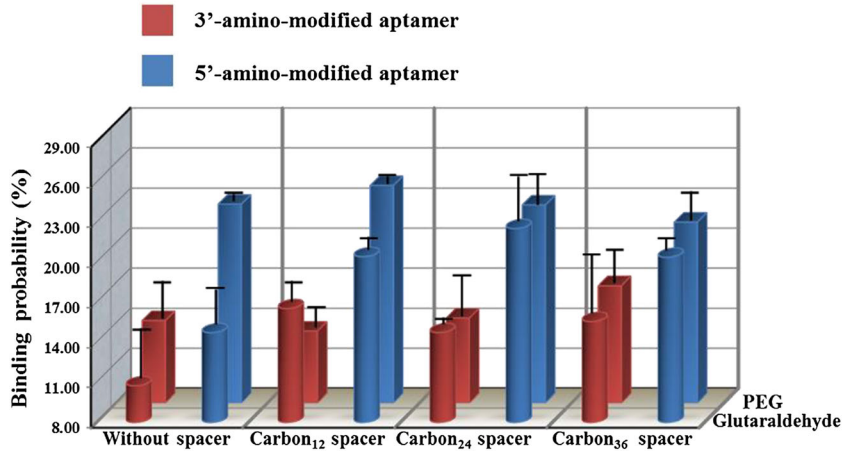

Figure 7. Effect of dodecyl spacer on the binding probability of 3′- or 5′-amino-modified aptamer/Bel-7404 cell. The constant loading rate was 3.4×10^5 pN/s. PEG, polyethylene glycol.

probability of aptamer/Bel-7404 cell slightly increased along with the length of dodecyl spacer increasing. As the length of dodecyl spacer increased up to carbon$_{12}$, the binding probability value almost reached the maximum (Figure 7). Moreover, an oligo(dT) was more effective than a dodecyl spacer and could improve the binding probability obviously. Take the immobilization of aptamer through its 3′-end using glutaraldehyde as the cross-linker for example, the T_{20} spacer with a length of 6.80 nm resulted in the binding probability increasing from $10.73 \pm 4.20\%$ to $20.83 \pm 3.85\%$, whereas the carbon$_{36}$ spacer with a length of 6.74 nm only resulted in the binding probability increasing from $10.73 \pm 4.20\%$ to $15.56 \pm 5.04\%$ (shown in Table S2 and Figure S1). It suggested that the length is not the most predominant factor in aptamer spacer design.

Evaluation of the specificity of immobilized aptamer

Besides affinity, the specificity of aptamer is also of great importance. According to the previous results, the binding probability of aptamer/Bel-7404 cell was relatively high when T_{20} spacer was incorporated into the aptamer at its 5′-end and PEG was used as the cross-linker. Therefore, such aptamer

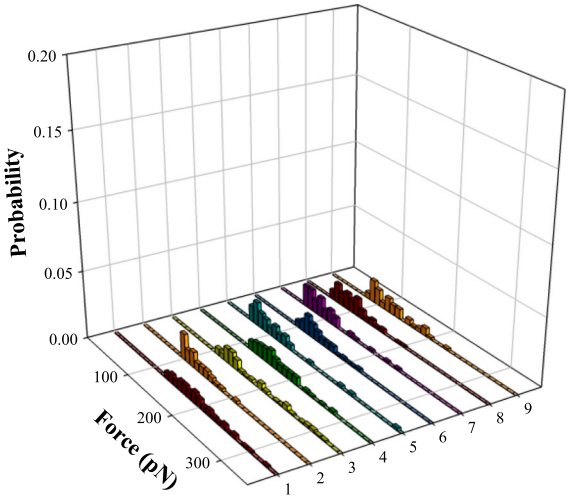

Figure 8. Force distribution of 5′-T_{20}-ls2n functionalized atomic force spectroscopy tip toward (1) Bel-7404 cell, (2) SMMC-7721 cell, (3) QBC-939 cell, (4) L-02 cell, and (5) HeLa cell. Polyethylene glycol was used as the cross-linker here. The constant loading rate was 3.4×10^5 pN/s.

was chosen to assess the specificity of aptamer toward Bel-7404 cell. Four kinds of cells including SMMC-7721 cell, QBC-939 cell, L-02 cell, and HeLa cell were chosen as control cells, and the interaction between control cells and 5′-amino-modified aptamer with T_{20} spacer was measured. As shown in Figure 8, in contrast to the binding probability of aptamer/Bel-7404 cell (28.95 ± 1.52%), the binding probability of aptamer/control cells decreased obviously, which were nearly in accordance with the binding probability between aptamer-functionalized AFM tip and blank substrate. Similarly, the binding probabilities of random DNA/Bel-7404 cell and random DNA/control cells were also low. The significant decrease of the binding probability and the random force distribution of these control experiments system demonstrated the specific interaction between aptamer and Bel-7404 cell. It suggested that such immobilization strategy did not influence the specificity of aptamer.

CONCLUSIONS

In conclusion, the effect of aptamer immobilization strategies on the interaction between immobilized aptamer and Bel-7404 cell has been systematically investigated using SMFS at the living cell level. Because SMFS explores the information about intrinsic properties of individuals, the effect of the surface density of aptamer can be negligible, thus resulting in the decreased complexity in studying the effect of aptamer immobilization strategies. The results showed that the biophysical characteristics of the aptamer at the molecular level remain undisturbed regardless of the change of immobilization strategies because similar unbinding force was maintained. However, the immobilization orientation, immobilization method, and linker could affect the binding probability of aptamer to its target cell. For aptamer/Bel-7404 cell, immobilization through 5′-end was superior to immobilization through 3′-end. Incorporating oligo(dT) spacer into aptamer at its 3′-end or 5′-end could dramatically improve the binding probability of aptamer/Bel-7404 cell when either PEG or glutaraldehyde was used as the cross-linker, whereas a dodecyl spacer could slightly improve the affinity of aptamer to Bel-7404 cell only for glutaraldehyde immobilization. Thus, a negatively charged oligo(dT) spacer was much more effective than a dodecyl spacer. In addition, PEG immobilization was superior to glutaraldehyde immobilization regardless of immobilization orientation and different spacers. These results are expected to provide essential information for further aptamer application in cell research.

Acknowledgements

This work was supported by the National Natural Science Foundation of China (21190040, 21375034, and 21175035), National Basic Research Program (2011CB911002), International Science and Technology Cooperation Program of China (2010DFB30300), and the Fundamental Research Funds for the Central Universities.

REFERENCES

Ali WH, Pichon V. 2014. Characterization of oligosorbents and application to the purification of ochratoxin A from wheat extracts. *Anal. Bioanal. Chem.* **406**: 1233–1240.

Balamurugan S, Obubuafo A, Soper SA, McCarley RL, Spivak DA. 2006. Designing highly specific biosensing surfaces using aptamer monolayers on gold. *Langmuir* **22**: 6446–6453.

Balamurugan S, Obubuafo A, Soper SA, Spivak DA. 2008. Surface immobilization methods for aptamer diagnostic applications. *Anal. Bioanal. Chem.* **390**: 1009–1021.

Baldrich E, Restrepo A, O'Sullivan CK. 2004. Aptasensor development: elucidation of critical parameters for optimal aptamer performance. *Anal. Chem.* **76**: 7053–7063.

Balic M, Williams A, Lin H, Datar R, Cote RJ. 2013. Circulating tumor cells: from bench to bedside. *Ann. Rev. Med.* **64**: 31–44.

Bell GI. 1978. Models for the specific adhesion of cells to cells. *Science* **200**: 618–627.

Bini A, Minunni M, Tombelli S, Centi S, Mascini M. 2007. Analytical performances of aptamer-based sensing for thrombin detection. *Anal. Chem.* **79**: 3016–3019.

Butt HJ, Jaschke M. 1995. Calculation of thermal noise in atomic force microscopy. *Nanotechnology* **6**: 1–7.

Cho EJ, Collett JR, Szafranska AE, Ellington AD. 2006. Optimization of aptamer microarray technology for multiple protein targets. *Anal. Chim. Acta* **564**: 82–90.

Eckel R, Wilking SD, Becker A, Sewald N, Ros R, Anselmetti D. 2005. Single-molecule experiments in synthetic biology: an approach to the affinity ranking of DNA-binding peptides. *Angew. Chem. Int. Ed.* **44**: 3921–3924.

Fang XH, Tan WH. 2009. Aptamers generated from cell-SELEX for molecular medicine: a chemical biology approach. *Acc. Chem. Res.* **43**: 48–57.

Formosa C, Lachaize V, Galés C, Rols MP, Martin-Yken H, François JM, Duval RE, Dague E. 2015. Mapping HA-tagged protein at the surface of living cells by atomic force microscopy. *J. Mol. Recognit.* **28**: 1–9.

Guo Q, Liu X, Tan Y, Wang K, Yang X, Zhou Y, Ye L, Zhao X. 2013. Selection of aptamers for human hepatocellular carcinoma with high specificity. *Chin. Sci. Bull.* **58**: 2745–2750.

Guo Z, Guilfoyle RA, Thiel AJ, Wang R, Smith LM. 1994. Direct fluorescence analysis of genetic polymorphisms by hybridization with oligonucleotide arrays on glass supports. *Nucleic Acids Res.* **22**: 5456–5465.

Jin Y, Wang K, Tan W, Wu P, Wang Q, Huang H, Huang S, Tang Z, Guo Q. 2004. Monitoring molecular beacon/DNA interactions using atomic force microscopy. *Anal. Chem.* **76**: 5721–5725.

Katilius E, Flores C, Woodbury NW. 2007. Exploring the sequence space of a DNA aptamer using microarrays. *Nucleic Acids Res.* **35**: 7626–7635.

Khezrian S, Salimi A, Teymourian H, Hallaj R. 2013. Label-free electrochemical IgE aptasensor based on covalent attachment of aptamer onto multiwalled carbon nanotubes/ionic liquid/chitosan nanocomposite modified electrode. *Biosens. Bioelectron.* **43**: 218–225.

Kienberger F, Ebner A, Gruber HJ, Hinterdorfer P. 2006. Molecular recognition imaging and force spectroscopy of single biomolecules. *Acc. Chem. Res.* **39**: 29–36.

Lao YH, Peck K, Chen LC. 2009. Enhancement of aptamer microarray sensitivity through spacer optimization and avidity effect. *Anal. Chem.* **81**: 1747–1754.

Luo L, Zhang Z, Ding Y, Deng D, Zhu X, Wang Z. 2013. Label-free electrochemical impedance genosensor based on 1-aminopyrene/grapheme hybrids. *Nanoscale* **5**: 5833–5840.

Panorchan P, George JP, Wirtz D. 2006. Probing intercellular interactions between vascular endothelial cadherin pairs at single-molecule resolution and in living cells. *J. Mol. Biol.* **358**: 665–674.

Schwarzenbach H, Nishida N, Calin GA, Pantel K. 2014. Clinical relevance of circulating cell-free microRNAs in cancer. *Nat. Rev. Clin. Oncol.* **11**: 145–156.

Shan YP, Wang HD. 2015. The structure and function of cell membranes examined by atomic force microscopy and single-molecule force spectroscopy. *Chem. Soc. Rev.* **44**: 3617–3638.

Shi H, Cui W, He X, Guo Q, Wang K, Ye X, Tang J. 2013. Whole cell-SELEX aptamers for highly specific fluorescence molecular imaging of carcinomas *in vivo*. *PLoS One* **8**: e70476.

Steffens C, Leite FL, Bueno CC, Manzoli A, Herrmann PSD. 2012. Atomic force microscopy as a tool applied to nano/biosensors. *Sensors* **12**: 8278–8300.

Tan W, Donovan MJ, Jiang J. 2013. Aptamers from cell-based selection for bioanalytical applications. *Chem. Rev.* **113**: 2842–2862.

Walter JG, Kökpinar O, Friehs K, Stahl F, Scheper T. 2008. Systematic investigation of optimal aptamer immobilization for protein-microarray applications. *Anal. Chem.* **80**: 7372–7378.

Wang C, Yadavalli VK. 2014. Investigating bimolecular recognition at the cell surface using atomic force microscopy. *Micron* **60**: 5–17.
Wang C, Yadavalli VK. 2014. Spatial recognition and mapping of proteins using DNA aptamers. *Nanotechnology* **25**: 455101.
Wang Q, Liu L, Yang X, Wang K, Chen N, Zhou C, Luo B, Du S. 2015. Evaluation of medicine effects on the interaction of myoglobin and its aptamer or antibody using atomic force microscopy. *Anal. Chem.* **87**: 2242–2248.
Wang Q, Zhou C, Yang X, Wang K, Liu L. 2014. Probing interactions between human lung adenocarcinoma A549 cell and its aptamers at single-molecule resolution. *J. Mol. Recognit.* **27**: 676–682.
Yang L, Wang K, Tan W, Li H, Yang X, Ma C, Tang H. 2007. Using force spectroscopy analysis to improve the properties of the hairpin probe. *Nucleic Acids Res.* **35**: e145.
Zhang XJ, Yadavalli VK. 2011. Surface immobilization of DNA aptamers for biosensing and protein interaction analysis. *Biosens. Bioelectron.* **26**: 3142–3147.
Zhao X, Wu J, Liang J, Yan J, Zhu Z, Yang CYJ, Mao B. 2012. Single-molecule force spectroscopic studies on intra- and intermolecular interactions of G-quadruplex aptamer with target Shp2 protein. *J. Phys. Chem. B* **116**: 11397–11404.
Zhao W, Cai M, Xu H, Jiang J, Wang H. 2013. A single-molecule force spectroscopy study of the interactions between lectins and carbohydrates on cancer and normal cells. *Nanoscale* **5**: 3226–3229.

SUPPORTING INFORMATION

Additional supporting information may be found in the online version of this article at the publisher's web site.